

# The potential of the sea breeze for wind energy generation in peri-urban coastal areas using small wind turbines

J. I. Rojas<sup>1</sup>, B. Cabrera<sup>2</sup>, J. Mazón<sup>3</sup>

1) Dept. of Physics – Division of Aerospace Eng., *Universitat Politècnica de Catalunya*, Castelldefels, Spain

2) EETAC, *Universitat Politècnica de Catalunya*, Castelldefels, Spain

3) Dept. of Physics, *Universitat Politècnica de Catalunya*, Castelldefels, Spain

Correspondence to: J. I. Rojas ([josep.ignasi.rojas@upc.edu](mailto:josep.ignasi.rojas@upc.edu))

## Abstract

This work investigates the potential of the sea breeze for wind energy generation with small wind turbines. For this purpose, we used wind data recorded in the Llobregat Delta (NE of the Iberian Peninsula) from 1993 to 2010 and turbine power curves obtained from QBlade, FAST and AeroDyn freeware tools, and from the manufacturer. The HP-600W turbine, with hub-height 8 m, would deliver 126 kWh in a year (53 kWh during the sea breeze period, i.e., March 1 to September 30, 10 to 19h LT), with average power of 14 W (27 W). The results for the entire year agree with data measured *in situ* in 2015, but it is not the case for the sea breeze period. Therefore, more research is necessary to validate completely the proposed approach, and to confirm the real potential of the sea breeze for micro-generation in a peri-urban coastal area like the one under study, where large wind farms are not feasible.

## 1 Introduction

Wind energy is one of the most promising renewable energy, obtained usually from wind farms installed in areas with significant synoptic winds (i.e., winds associated with the meteorological macroscale). These wind farms typically use large wind turbines (tower height  $\geq 80$  m), with high efficiency in converting kinetic energy of horizontal synoptic wind into

1 electricity. However, urban and suburban areas –where local, weaker winds (thermal winds)  
2 are generally dominant– are receiving increasing attention as potential sites for wind energy  
3 generation using small wind turbines (SWT). Recent investigations on local wind regimes  
4 [1]–[4] and wind farms in coastal sites [5]–[7] have enabled better assessment of the wind  
5 resource. However, simulations of wind energy generated from local winds are scarce. An  
6 exception is a work comparing the sea breeze in the US Middle Atlantic Bight with synoptic  
7 winds from data for 18 years [8], concluding that, while the average wind speed was below  
8  $5.7 \text{ m s}^{-1}$ , the sea breeze is suitable for daily energy generation in the studied coastal area.

9         The objectives of this work are: 1) investigate the potential of the sea breeze for wind  
10 energy generation; 2) quantify the power production by SWT in the Llobregat Delta (NE of  
11 the Iberian Peninsula); 3) compare the production during the sea breeze period (March 1 to  
12 September 30, 10 to 19h LT) with that for a reference year; and 4) validate the performance of  
13 QBlade, FAST and AeroDyn simulation tools.

## 14 **1.1 The sea breeze**

15         The sea breeze is a thermal circulation showing diurnal cycle in the local scale [9]–  
16 [13]. It appears in coastal areas due to the differences between the air over the land and the  
17 sea during daytime, particularly in warmer months: the air over the land is heated faster, and  
18 gains altitude, while the air over the sea moves inland forming a cold front. The air over the  
19 land that gained altitude travels hundreds of kilometers offshore, where a subsidence occurs,  
20 closing the thermal cycle. The sea breeze layer thickness ranges from 50 m (at dawn) to 300–  
21 400 m [9]. The sea breeze is usually weaker than synoptic winds, but features larger  
22 periodicity and high predictability, which is most interesting. The direction of the sea breeze  
23 rotates due to the Coriolis force (in the northern hemisphere, it turns clockwise). In the  
24 Llobregat Delta, the sea breeze blows from the SE (SW) at the beginning (end) of the day. At  
25 night, a reversed thermal circulation appears (the land breeze, usually less intense).

26

## 27 **2 Methods and materials**

28         Two coupled freeware tools from the National Renewable Energy Laboratory were  
29 used to obtain the turbine power curves: FAST v7.01, a dynamics analysis code for

1 computing the loads on horizontal-axis wind turbines (HAWT) [14]; and AeroDyn v13.00, an  
2 aerodynamics analysis code that, together with a dynamics code, computes aerodynamic loads  
3 on blade elements [15] and the behavior of control and protection systems and structural  
4 dynamics of HAWT [16]. FAST and AeroDyn have been applied in many investigations [16];  
5 namely, these codes were assessed by *Germanischer Lloyd WindEnergie* and found adequate  
6 for design and certification of onshore HAWT [17]. These tools require input data like the  
7 wind conditions and blade parameters. The latter can be obtained from technical data by the  
8 manufacturer or from measuring physical components, e.g., by 3D digitalization of a blade.

9 QBlade, an open source software for design and simulation of HAWT, distributed  
10 under the GNU General Public License, was also used. XFOIL, integrated within QBlade,  
11 allows airfoil design and performance analysis. In addition, QBlade allows for extrapolation  
12 of airfoil performance data to 360° angle of attack, turbine blade design, realization of rotor  
13 and turbine simulations, structural blade design, modal and static load analyses using QFem  
14 solver, generation of turbulent windfields, and realization of FAST simulations.

15 Two off-grid SWT (the IT-PE-100 and HP-600W; see the technical specifications in  
16 Table 1) were selected for this research because: 1) the start-up<sup>1</sup> wind speed,  $V_{su}$ , and cut-in<sup>2</sup>  
17 wind speed,  $V_{ci}$ , are relatively low (3 and 3.5 m s<sup>-1</sup>), which makes them suitable for weak  
18 winds like the sea breeze; 2) their size is relatively small, which makes them suitable for  
19 urban/suburban areas, and areas close to an airport; and 3) we installed the HP-600W in the  
20 studied area, and we plan to install also the IT-PE-100.

21 The IT-PE-100 was designed by ITDG for communities in remote areas of developing  
22 countries following the appropriate technology philosophy [18], [19]. The IT-PE-100 is not  
23 patented, and manuals, design specifications, and technical data are open-access [20], [21].  
24 The blades and the hub are made of glass fiber reinforced polymer, and thus are light but with  
25 good structural properties. The turbine operates at high rotational speeds, which allows direct  
26 connection of the rotor shaft to the generator shaft without a heavy transmission system [22].  
27 The nacelle, a cylindrical piece of steel in the tower's upper end to which the generator-rotor  
28 system is attached, allows rotation around the vertical axis, facilitating the alignment with the  
29 incident wind.

---

<sup>1</sup> The start-up speed is the wind speed at which an unloaded rotor starts turning.

<sup>2</sup> The cut-in speed is the wind speed at which a wind turbine starts pushing power into the battery bank or the grid.

1 The HP-600W, developed by Hopeful Energy, is light, compact and smaller than most  
2 low-wind speed turbines and SWT. The blades are made of nylon and glass fiber reinforced  
3 polymer coated to prevent problems due to corrosion, high temperatures, water, salinity, dust  
4 and sand. It works at higher nominal wind speed and rotational speed than the IT-PE-100, but  
5 both have axial-flux permanent magnet synchronous generator [22], [23].

### 7 3 Results and discussion

#### 8 3.1 Wind speed distribution and prevailing wind direction

9 A weather station of the Catalan Weather Service (MeteoCat) has been measuring  
10 wind data in the Llobregat Delta since 1993. Every 10 min, the station averages and records  
11 the wind speed at 2 m high. The data available to the users are the hourly averages of these  
12 records<sup>3</sup>. Assuming a stable atmosphere and a roughness length  $z_0$  of 0.25, corresponding to  
13 open landscape and areas with scattered shelter belts [24], the wind speed at 8, 10 and 15 m  
14 was computed from the weather station data using the potential wind equation (Eq. 1):

$$15 \quad V_H = V_{2m} \frac{\ln(\frac{H}{z_0})}{\ln(\frac{2}{z_0})} \quad (1)$$

16 where  $V_H$  is the velocity at a height  $H$ , and  $V_{2m}$  is the wind speed at 2 m. The Weibull  
17 probability density function was fitted to the extrapolated data from 1993 to 2010. Fig. 1 and  
18 Fig. 2 show, respectively, the Weibull distributions for the wind speed at 10 m for the entire  
19 year and for the sea breeze period. The former (latter) has a shape factor,  $k$ , of 1.51 (1.80)<sup>4</sup>  
20 and a scale factor,  $C$ , of 3.01 (4.23); the probability for  $V_H > 3 \text{ m s}^{-1}$  is 36.9% (58.4%), that is  
21 3232 hours per year and 1250 hours during the sea breeze period.

22 Finally, wind directions ranging from NW to NE represent 45% of the total  
23 measurements for the entire year in the Llobregat Delta, while wind directions ranging from  
24 SW to SE represent 38%. Considering the sea breeze period, the dominant direction is SW,

---

<sup>3</sup> If abundant reliable measurements of wind speed in the geographical area of study were not available, an alternative is to use wind speed predictions using the well accepted tools for micro-scale wind resource assessment [30], [31], like WRF or also NEWA, in the short-term future. The use of these tools is a de-facto standard, for example, in wind farm design [32].

<sup>4</sup>  $k \approx 2$  is usual in north European sites, e.g., in good rural and high rise sites [25].

1 clearly corresponding to the sea breeze circulation. Thus, it can be assumed that the wind  
2 energy generated during the sea breeze period is basically due to the sea breeze.

### 3 **3.2 Power curves**

4 Fig. 3 and Fig. 4 show the power curves obtained from QBlade, FAST and AeroDyn  
5 and the manufacturer for the IT-PE-100 and HP-600W, respectively, and the Weibull curves  
6 from Sect. 3.1. The relative error between power curves (associated with inaccuracies and  
7 limitations of the models used by FAST and AeroDyn, the turbine models, and the power  
8 curves from the manufacturer) is  $10.1 \pm 13.3\%$  for the IT-PE-100 and  $-28.4 \pm 2.9\%$  for the  
9 HP-600W, for which the simulated power is lower than the manufacturer data (suppliers of  
10 commercial turbines typically provide over-optimistic performance data of their products).  
11 From the simulations, the IT-PE-100 produces more power than the HP-600W at low wind  
12 speeds, while the contrary occurs if we consider the manufacturer data. The average error is  
13 larger for the HP-600W, as expected, since less design and technical data for the proper  
14 modeling of this commercial turbine was available. The power curves agree more closely with  
15 manufacturer data at low wind speeds, while a tailing off is observed at high wind speeds  
16 [25]. The power curve from QBlade shows deviations from the manufacturer data, with power  
17 being underestimated (overestimated) below (above) a wind speed of  $\approx 6$  m/s.

### 18 **3.3 Average power and overall energy produced**

19 Among the methods to obtain the probability distribution of the power produced, the  
20 static method is the simplest, as it ignores non-stationary effects, i.e., losses due to changes in  
21 wind direction and maintenance periods [26]. It assumes that the probability density function  
22 of the power produced is a Weibull curve identical to that corresponding to the wind speed  
23 distribution. Hence, the probability for the turbine to provide a given power comes from  
24 superposing the power curve,  $P_{turb}(V)$ , and the Weibull distribution of the wind speed,  $f(V)$ , as  
25 shown in Fig. 3 and Fig. 4. The average power,  $P_{ave}$ , computed with the static method (Eq. 2;  
26 where  $V_{ci}$  and  $V_{co}$  are the cut-in and cut-out speeds from Table 1) and overall energy,  $E$ ,  
27 produced by the SWT in the entire year and in the sea breeze period are shown in Table 2.

$$28 \quad P_{ave} = \int_{V_{ci}}^{V_{co}} P_{turb}(V) f(V) dV \quad (2)$$

1           The values in Table 2 are similar to those from the Warwick Wind Trials Project [25],  
2 which measured the energy generated by building-mounted, grid connected SWT in 26  
3 different sites [27]. The average wind speed ranged from 1.7 to 6.7 m s<sup>-1</sup>, and the average  
4 annual energy produced per turbine was 78 kWh. If not taking into account the periods with  
5 the turbines switched off, the average was 230 kWh per year (94 kWh per year if omitting the  
6 results for the best site and highest buildings). The turbine in the poorest site produced 15  
7 kWh per year in average, less than the energy consumed by the turbine's electronics.

8           In Table 2, the results for the entire year using the simulated power curve of the HP-  
9 600W and the wind speed measured from 1993 to 2010 agree with the *in situ* measurements  
10 in 2015, as shown in Table 3; namely, the average power is 14 vs 13 W and the produced  
11 energy is 126 vs 100 kWh. These data are statistically significant because in 2015 the data  
12 acquisition system was operative 292 days, i.e., 80.0% of the year. However, the *in situ*  
13 measurements in 2016 are not representative because the data acquisition system has been  
14 operative only 126 days, i.e., 34.5% of the year, all of which are within the spring and the  
15 summer, not homogeneously distributed throughout the year. If using the manufacturer power  
16 curve instead of the simulated curves, the results in 2015 overestimate a little more the power  
17 and energy (this is expected since manufacturer power curves are typically over-optimistic).  
18 However, it is important to recall that, since the measured wind speed data and manufacturer  
19 power curves are often not very accurate, it is not uncommon to obtain energy predictions  
20 with errors larger than ±25% if data is not significantly pre-processed; e.g., energy outputs  
21 overestimated by a factor between 1.7 and 3.4 have been reported in previous works [25].

22           Unfortunately, the *in situ* measurements for the sea breeze period in both 2015 and  
23 2016 are significantly below our predictions. In this case, the data acquisition system was  
24 operative 207 and 126 days, i.e., 96.7% and 58.9% of the sea breeze period, respectively.  
25 Thus, more research and longer data series are necessary to establish the real potential of the  
26 sea breeze in the studied location.

#### 27 **4 Conclusions**

28           This work investigates the potential of the sea breeze for wind energy generation with  
29 SWT (the IT-PE-100 and HP-600W), using as case study the Llobregat Delta (NE of the  
30 Iberian Peninsula). For this purpose, we applied the static method using wind data recorded *in*

1 *situ* from 1993 to 2010 and turbine power curves obtained from QBlade, FAST and AeroDyn  
2 freeware tools, and from the manufacturer. The following conclusions are drawn:

- 3 • The predicted annual energy ranges from 111 to 312 kWh, depending on the  
4 wind turbine, the hub-height and whether we use the manufacturer power curve  
5 or the simulated power curve.
- 6 • 42% to 55% of this energy is generated during the sea breeze period (March 1  
7 to September 30, 10 to 19h LT), which is 22% of the total time in a year.
- 8 • The results for the entire year agree with data measured *in situ* in 2015, but it is  
9 not the case for the sea breeze period. Thus, more research and longer data  
10 series are necessary to validate completely the proposed approach, and to  
11 confirm the real potential of the sea breeze for micro-generation in a peri-urban  
12 coastal area like the one under study, where large wind farms are not feasible.
- 13 • This work tested the suitability of FAST and AeroDyn for simulation of SWT  
14 operating in low-wind speed conditions. For the IT-PE-100, the simulated  
15 power curve and the manufacturer power curve compare well. It may not seem  
16 so for the HP-600W, but many technical data essential for the proper modeling  
17 of the turbine was lacking.
- 18 • The Llobregat Delta is a suburban area, characterized by presence of farms,  
19 secondary roads and paths between cities, and a 20 km long promenade  
20 following the coastline. The SWT have small rotor diameters, and hub-heights  
21 equivalent to a street light, and thus could be installed in lighting systems  
22 besides roads, paths and the long promenade. Besides feeding the lighting  
23 systems, the energy could be used for many purposes, like feeding electric  
24 pumps for farmers to extract water from the aquifer to water crops [28], [29].

## 25 26 **Acknowledgements**

27 The authors thank the valuable help from undergraduate students Carlos Sánchez,  
28 Jordi Jou, Aaron Valle and David Olmeda.

## References

- [1] S. Bivona, R. Burlon, and C. Leone, “Hourly wind speed analysis in Sicily,” *Renew. Energy*, vol. 28, no. 9, pp. 1371–1385, 2003.
- [2] J. A. Carta and P. Ramirez, “Analysis of two-component mixture Weibull statistics for estimation of wind speed distributions,” *Renew. Energy*, vol. 32, no. 3, pp. 518–531, 2007.
- [3] A. N. Celik, A. Makkawi, and T. Muneer, “Critical evaluation of wind speed frequency distribution functions,” *J. Renew. Sustain. Energy*, vol. 2, no. 1, p. 13102, 2010.
- [4] A. W. Dahmouni, M. Ben Salah, F. Askri, C. Kerkeni, and S. Ben Nasrallah, “Wind energy in the Gulf of Tunis, Tunisia,” *Renew. Sustain. Energy Rev.*, vol. 14, no. 4, pp. 1303–1311, 2010.
- [5] G. J. Dalton, D. A. Lockington, and T. E. Baldock, “Feasibility analysis of stand-alone renewable energy supply options for a large hotel,” *Renew. Energy*, vol. 33, no. 7, pp. 1475–1490, 2008.
- [6] A. Montlaur, S. Cochard, and D. F. Fletcher, “Formation of tip-vortices on triangular prismatic-shaped cliffs. Part 2: A computational fluid dynamics study,” *J. Wind Eng. Ind. Aerodyn.*, vol. 109, pp. 21–30, 2012.
- [7] M. S. Mason, G. S. Wood, and D. F. Fletcher, “Numerical investigation of the influence of topography on simulated down burst wind fields,” *J. Wind Eng. Ind. Aerodyn.*, vol. 98, pp. 21–33, 2010.
- [8] R. W. Garvine and W. Kempton, “Assessing the wind field over the continental shelf as a resource for electric power,” *J. Mar. Res.*, vol. 66, no. 6, pp. 751–773, 2008.
- [9] J. E. Simpson, *Sea Breeze and Local Winds*. Cambridge, UK: Cambridge University Press, 1994.
- [10] R. Rotunno, “On the linear-theory of the land and sea breeze,” *J. Atmos. Sci.*, vol. 40, no. 8, pp. 1999–2009, 1983.
- [11] M. A. Estoque, “A theoretical investigation of the sea breeze,” *Q. J. R. Meteorol. Soc.*, vol. 87, no. 372, pp. 136–146, 1961.



- 1 [12] D. G. Steyn and G. Kallos, “A study of the dynamics of hodograph rotation in the sea  
2 breezes of Attica, Greece,” *Boundary-Layer Meteorol.*, vol. 58, no. 3, pp. 215–228,  
3 1992.
- 4 [13] R. W. Arritt, “Effects of the large-scale flow on characteristic features of the sea  
5 breeze,” *J. Appl. Meteorol.*, vol. 32, no. 1, pp. 116–125, 1993.
- 6 [14] J. M. Jonkman and M. L. Buhl, “FAST User’s Guide – Technical Report NREL/EL-  
7 500-38230.” National Renewable Energy Laboratory (NREL), Golden, CO, USA,  
8 2005.
- 9 [15] D. J. Laino and A. C. Hansen, “User’s Guide to the Wind Turbine Dynamics  
10 Aerodynamics Computer Software AeroDyn.” Woodward Engineering, LLC, Salt Lake  
11 City, UT, USA, 2002.
- 12 [16] J. M. Jonkman and D. Matha, “Dynamics of offshore floating wind turbines-analysis of  
13 three concepts,” *Wind Energy*, vol. 14, no. 4, pp. 557–569, 2011.
- 14 [17] A. Manjock, “Evaluation Report: Design Codes FAST and ADAMS® for Load  
15 Calculations of Onshore Wind Turbines – Report No. 72042,” Germanischer Lloyd  
16 WindEnergie GmbH, Humburg, Germany, RPRT, 2005.
- 17 [18] L. Ferrer-Marti, A. Garwood, J. Chiroque, R. Escobar, J. Coello, and M. Castro, “A  
18 community small-scale wind generation project in Peru,” *Wind Eng.*, vol. 34, no. 3, pp.  
19 277–288, 2010.
- 20 [19] L. Ferrer-Marti, A. Garwood, J. Chiroque, B. Ramirez, O. Marcelo, M. Garfi, and E.  
21 Velo, “Evaluating and comparing three community small-scale wind electrification  
22 projects,” *Renew. Sustain. Energy Rev.*, vol. 16, no. 7, pp. 5379–5390, 2012.
- 23 [20] H. Piggott, “The Permanent Magnet Generator (PMG): A manual for manufacturers  
24 and developers.” Scoraig Wind Electric, Scotland, UK, p. 27, 2001.
- 25 [21] T. Sanchez, S. Fernando, and H. Piggott, “Wind rotor blade construction - Small wind  
26 systems for battery charging.” ITDG, UK, p. 51, 2001.
- 27 [22] A. Colet-Subirachs, O. Gomis-Bellmunt, D. Clos-Costa, G. Martin-Segura, A. Junyent-  
28 Ferre, R. Villafafila-Robles, and L. Ferrer-Marti, “Electromechanical modelling and  
29 control of a micro-wind generation system for isolated low power DC micro grids,”

- 1           *Eur. Power Electron. Drives Assoc. J.*, vol. 20, no. 2, pp. 42–48, 2010.
- 2 [23] J. F. Gieras, R. J. Wang, and M. J. Kamper, *Axial Flux Permanent Magnet Brushless*  
3           *Machines*, 1st ed., vol. 3 ed. Dordrecht, The Netherlands: Springer Netherlands, 2004.
- 4 [24] H. Moalic, J. A. Fitzpatrick, and A. A. Torrance, “The correlation of the characteristics  
5           of rough surfaces with their friction coefficients,” *Proc. Inst. Mech. Eng. Part C-*  
6           *Journal Mech. Eng. Sci.*, vol. 201, no. 5, pp. 321–329, 1987.
- 7 [25] D. Hailes, “Warwick Wind Trials Project (WWTP) final report,” Encraft, Warwick,  
8           UK, RPRT, 2009.
- 9 [26] T. Burton, D. Sharpe, N. Jenkins, and E. Bossanyi, *Wind Energy Handbook*, vol. 2 ed.  
10           Chichester, UK: John Wiley & Sons, Ltd., 2011.
- 11 [27] R. Walters and P. R. Walsh, “Examining the financial performance of micro-generation  
12           wind projects and the subsidy effect of feed-in tariffs for urban locations in the United  
13           Kingdom,” *Energy Policy*, vol. 39, no. 9, pp. 5167–5181, 2011.
- 14 [28] O. Ozgener, “Use of solar assisted geothermal heat pump and small wind turbine  
15           systems for heating agricultural and residential buildings,” *Energy*, vol. 35, no. 1, pp.  
16           262–268, 2010.
- 17 [29] A. M. De Broe, S. Drouilhet, and V. Gevorgian, “A peak power tracker for small wind  
18           turbine in battery charging applications,” *IEEE Trans. Energy Convers.*, vol. 14, no. 4,  
19           pp. 1630–1635, 1999.
- 20 [30] S. K. Khadem and M. Hussain, “A pre-feasibility study of wind resources in Kutubdia  
21           Island, Bangladesh,” *Renew. Energy*, vol. 31, no. 14, pp. 2329–2341, 2006.
- 22 [31] M. Ranaboldo, L. Ferrer-Marti, and E. Velo, “Micro-scale wind resource assessment  
23           for off-grid electrification projects in rural communities. A case study in Peru,” *Int. J.*  
24           *Green Energy*, vol. 11, pp. 75–90, 2014.
- 25 [32] L. Landberg, L. Myllerup, O. Rathmann, E. L. Petersen, B. H. Jorgensen, J. Badger,  
26           and N. G. Mortensen, “Wind resource estimation - An overview,” *Wind Energy*, vol. 6,  
27           no. 3, pp. 261–271, 2003.

28  
29

1 Table 1. Summary of technical data of the IT-PE-100 and the HP-600W wind turbines.

Concept	IT-PE-100	HP-600W
Rated output power	100 W	600 W
Rotor configuration	3 blades, upwind, HAWT	3 blades, upwind, HAWT
Control	Variable speed, furling tail	No information available
Blades	Fixed-pitch, NACA 4412 airfoils	No information available
Drive train	High speed, direct coupling	No information available
Rotor diameter	1.7 m	1.5 m
Blade length	0.7 m	0.68 m
Hub diameter	0.3 m	0.14 m
Hub-height	8 – 10 m	8 – 10 m
Start-up wind speed	3 m s <sup>-1</sup>	3 m s <sup>-1</sup>
Cut-in wind speed	3.5 m s <sup>-1</sup>	3.5 m s <sup>-1</sup>
Rated wind speed	6.5 m s <sup>-1</sup>	12 m s <sup>-1</sup>
Maximum wind speed	12 m s <sup>-1</sup>	25 m s <sup>-1</sup>
Rated rotor rotational speed	420 rpm	810 rpm

2

3

1 Table 2. Average power,  $P_{ave}$ , and energy,  $E$ , obtained with the static method (using a power  
2 curve from the manufacturer or FAST and AeroDyn) for the IT-PE-100, HP-600W  
3 and SP-500 for the sea breeze period (March 1 to September 30, 10 to 19h LT) and the  
4 entire year.

Power curve (turbine)	Period	Height 8 m		Height 10 m		Height 15 m	
		$P_{ave}$ [W]	$E$ [kWh]	$P_{ave}$ [W]	$E$ [kWh]	$P_{ave}$ [W]	$E$ [kWh]
Manufacturer (IT-PE-100)	Sea-breeze	28	53	33	63	43	83
	Entire year	14	123	15	132	21	180
Simulations (IT-PE-100)	Sea-breeze	28	53	35	67	48	93
	Entire year	13	111	14	121	21	180
Simulations (IT-PE-100) <sup>a</sup>	Sea-breeze	47	90	56	108	75	144
	Entire year	24	213	26	208	36	312
Manufacturer (HP-600W)	Sea-breeze	37	71	45	86	62	119
	Entire year	18	157	19	170	28	242
Simulations (HP-600W)	Sea-breeze	27	53	33	63	43	83
	Entire year	14	126	15	134	21	182
Manufacturer (SP-500) <sup>b</sup>	Sea-breeze	28	53	33	63	43	83
	Entire year	13	111	14	121	21	180

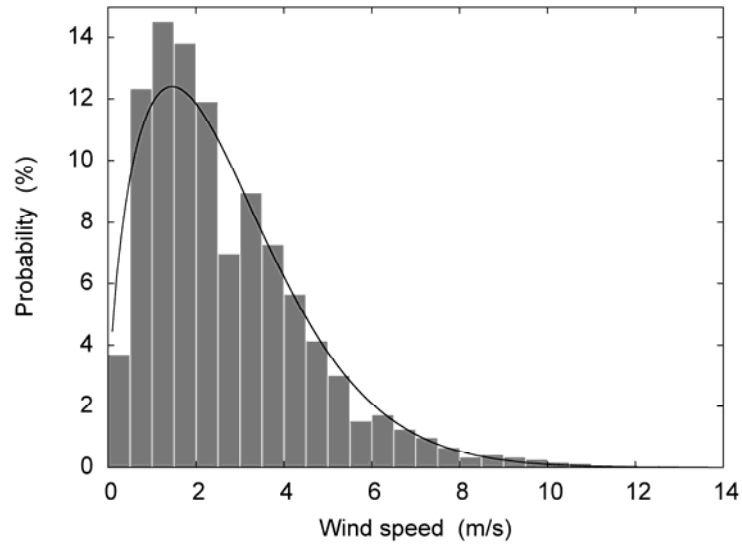
5 <sup>a</sup> These results correspond to the IT-PE-100 operating constantly at its peak power coefficient ( $\approx 0.37$ ) thanks to the simple  
6 open-loop control algorithm developed *ad hoc* by Colet-Subirachs et al. [18].

7 <sup>b</sup> The results for the SP-500 wind turbine, which is currently under development by ITDG, are only for informative purposes,  
8 since this large turbine is less appropriate than the IT-PE-100 for weak, low-speed wind regimes. The SP-500 is a 3-bladed,  
9 upwind HAWT, with rotor diameter 3 m and rated power 500 W at a rated wind speed of 8 m/s and rated rotational speed of  
10 300 rpm. The SP-500 is also an open access technology, like the IT-PE-100.  
11

1 Table 3. Average power,  $P_{ave}$ , and energy,  $E$ , obtained from *in situ* measurements in the  
 2 Agròpolis of Viladecans, in the Llobregat Delta, for the HP-600W for the sea breeze  
 3 period (March 1 to September 30, 10 to 19h LT) and the entire year.

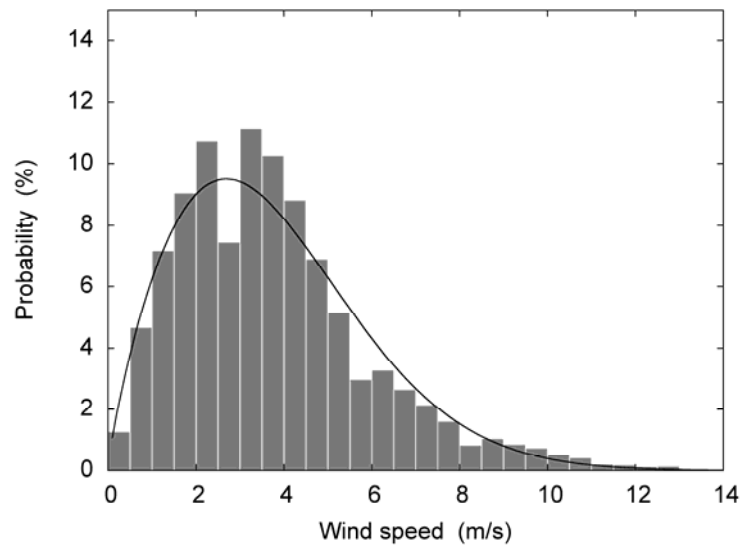
Year of tests (turbine)	Period	Height 8 m	
		$P_{ave}$ [W]	$E$ [kWh] <sup>a</sup>
Year 2015 (HP-600W)	Sea-breeze	9	14
	Entire year	13	100
Year 2016 (HP-600W)	Sea-breeze	10	19
	Entire year	5	42

4 <sup>a</sup> Since neither in 2015 nor 2016 we have *in situ* measurements of power for the entire year or for the entire sea breeze period,  
 5 the energy reported in this table is obtained assuming that, in the missing days for the corresponding time period, the power is  
 6 equal to the average power computed from the available data for that period.  
 7  
 8



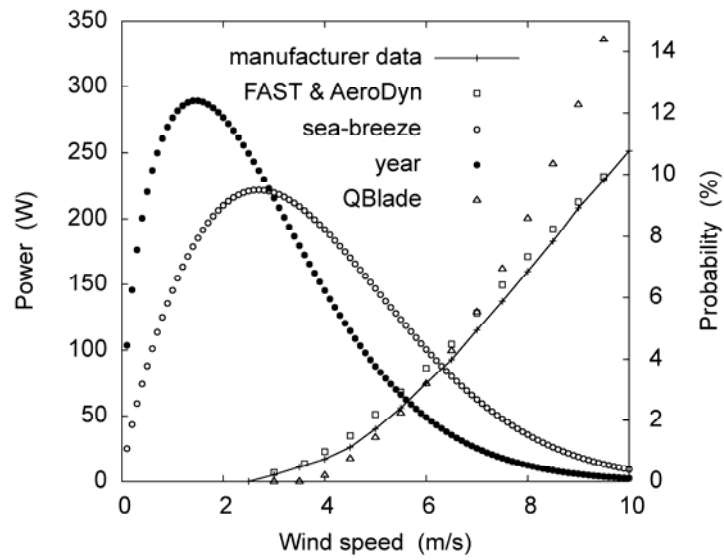
1  
2  
3  
4  
5  
6

Figure 1. Wind speed distribution and fitted Weibull probability density function for the entire year (January 1 to December 31, 00 to 24 LT) as obtained from wind speed data measured in the Llobregat Delta from 1993 to 2010.



1  
2  
3  
4  
5  
6

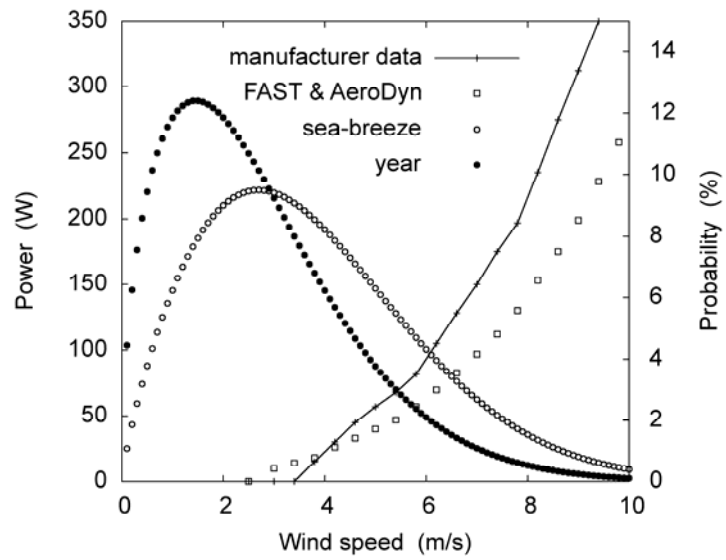
Figure 2. Wind speed distribution and fitted Weibull probability density function for the sea breeze period (March 1 to September 30, 10 to 19 LT) as obtained from wind speed data measured in the Llobregat Delta from 1993 to 2010.



1  
2  
3  
4  
5  
6  
7

Figure 3. For the IT-PE-100: manufacturer power curve and power curves obtained from FAST and AeroDyn, and from QBlade, together with Weibull distributions for the entire year and the sea breeze period (March 1 to September 30, 10 to 19 LT) as obtained from wind speed data measured in the Llobregat Delta from 1993 to 2010.





1  
2  
3  
4  
5  
6  
7

Figure 4. For the HP-600W: manufacturer power curve and power curve obtained from FAST and AeroDyn, together with Weibull distributions for the entire year and the sea breeze period (March 1 to September 30, 10 to 19 LT) as obtained from wind speed data measured in the Llobregat Delta from 1993 to 2010.